A Nonlinear Feedback Controller for a Single-Link Flexible Manipulator Based on a Finite Element Model

S. S. Ge,* T. H. Lee, and G. Zhu
Centre for Intelligent Control
Department of Electrical Engineering
National University of Singapore
10 Kent Ridge Crescent
Singapore 119260
e-mail: elegss@ee.nus.sg

Received May 11, 1995; revised August 19, 1996
accepted September 11, 1996

In this article, a nonlinear dynamic model of a flexible manipulator is derived through finite element method associated with Lagrange approach. The flexible manipulator is modeled as an Euler–Bernoulli beam driven by a motor at its base and with a point mass tip payload. The generalized coordinates of the system are selected to be the displacements and rotations of the nodes on the considered flexible beam, and such that a state space model is obtained with all the state variables having physical meanings. Based on this model, an effective nonlinear feedback controller is developed to control the tip position. Furthermore, an efficient algorithm is developed to calculate the inverse of the system's inertia matrix for real-time implementation. Numerical simulation results are given to show the effectiveness of the controller and its robustness in handling payload variations.

この発表では、フレキシブル・マニピュレータの非線型力学モデルを、ラグランジェ法に関連した有限要素法によって導出する。フレキシブル・マニピュレータは、その基台にあるモーターと点質量先端ペイロードによって駆動されるEuler - Bernoulliビームとしてモデル化される。システムの一般化された座標で、対象となるフレキシブル・ビームの上にあるノードの変位と回転を表すと、物理的に意味のあるすべての状態変数によって状態空間モデルを作成できる。このモデルに基づいて、先端位置を制御する、効果的な非線型フィードバック・コントローラを開発した。さらに、リアルタイム実装を行うためにシステムの慣性マトリックスの逆行列を計算する、有効なアルゴリズムを開発する。数値シミュレーションの結果を使って、様々なペイロードの変化におけるコントローラの有効性と堅牢性を証明する。

*To whom all correspondence should be addressed.

Journal of Robotic Systems 14(3), 165–178 (1997)

CCC 0741-2223/97/030165-14

1. INTRODUCTION

To overcome the drawbacks of today's industrial robots, such as large weights, high energy consumptions, and low speed operations, much research work[1–23] has been carried out in modeling and control of lightweight flexible manipulators.

The two most commonly used modeling methods are the Assumed Modes Method (AMM) and Finite Element Method (FEM). In ref. 1, the flexible beam was modeled using AMM under pinned-free boundary conditions, and a linear state-space model was obtained. The authors of ref. 2 gave a detailed modeling process of a flexible beam under clamped-free boundary conditions with AMM. Comparison studies between the above two linear AMM models were carried out in ref. 3, in which the conclusions were made that (1) the pinned-free model performs better than the clamped-free model when the hub inertia I_h is comparatively small, and (2) the two models match each other well when I_h is large.

Based on the linear clamped-free AMM model, a transfer function model of a flexible beam was discussed by Wang and Vidyasagar.[4] They proved that the transfer function between the net deflection (the sum of the rigid motion and the elastic deformation) and the control input is not well-defined when the number of modes approaches infinity. It was found that a modified output, which was defined to be the rigid motion minus the elastic deformation, can ensure the existence of a well-defined transfer function with a relative degree of two. The FEM modelling of flexible manipulators can be found in refs. 5, 6, and 19. Single-link flexible beams were considered in refs. 5 and 19, while multi-link flexible manipulators were discussed in ref. 6.

Much of the existing research work is carried out based on dynamic models obtained using AMM, in which the elastic deflection of the beam is represented by a series of separable modes. Although the AMM can give some physical insights into the system, such as the concept of natural frequencies, its generalized coordinates do not have any explicit physical meanings. On the other hand, FEM has its own advantages and disadvantages, such as all the generalized coordinates have physical meanings, but, the concept of natural frequencies is lost. A comparison studies between the two methods have been carried out in ref. 7. In this article, the controller is designed based on a FEM nonlinear model under the assumption that the states are obtainable.

Different control techniques have been investigated in the control of flexible robots. In ref. 3, a bounded H_2 input LQG compensator was designed based on a linear AMM model to control the tip position of a flexible beam. Input-shaping method was used in controlling a flexible beam in refs. 8 and 9. This method can effectively suppress the elastic vibrations of the flexible beam, but at the same time will slow down the transient response. Although input-shaping method is only valid for linear time-invariant (LTI) systems theoretically, satisfactory control results were obtained by combining it with an adaptive identification scheme to estimate the modal frequencies,[9] or with a linear PD controller and a rigid body inverse dynamics linearization process to form a closed-loop controller.[8] The dynamic model inversion technique, which is quite effective in controlling rigid manipulators, was also introduced into the flexible case in refs. 10 and 11. The authors of ref. 10 developed an efficient algorithm base on a FEM model to achieve on-line computation of desired open loop control torques. In ref. 11, the design of feed-forward controllers based on the discrete inverse dynamics technique was discussed, and an optimal scheme was introduced to minimize the integral square of the error between the reference input and the system's output. Singular perturbation theory has been found to be very effective in controlling flexible robots by decomposing the system into a fast subsystem and a slow subsystem, and stabilizing the two subsystems using a composite law.[12,13] To handle the changing parameters of the flexible beam system, various adaptive schemes, such as self-tuning control,[14,15] model reference adaptive control,[16,17] and other adaptive schemes,[18–22] were also introduced to control flexible manipulators. Comparison studies between the linear PD controller, LQR controller, feedback linearalization control, singular perturbation method, and sliding modes techniques were carried out in ref. 23 with respect to a single-link flexible robotic arm. It was found that singular perturbation method gives the best tracking performance of the reference trajectory. In this article, a nonlinear feedback controller is presented based on a FEM model to achieve tip position control. The controller can be shown to be very robust to the changes in tip payload, and the closed-loop system is proved to be asymptotically stable.

The rest of the article is organized as follows: Dynamic modeling based on FEM is given in section 2. The nonlinear controller design is presented in section 3, and in section 4, numerical simulation studies are provided, followed by the conclusion in section 5.

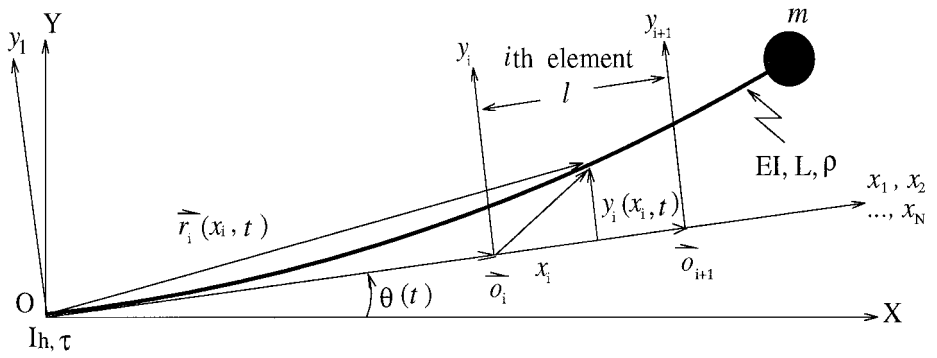

Figure 1. Finite element modeling of a flexible beam.

2. DYNAMIC MODELING BY FEM

The flexible manipulator, shown in Figure 1, is modeled as an *Euler-Bernoulli* beam clamped on the rotor of a motor. A torque applied by the motor rotates the beam in the horizontal plane without the gravitational influence. The beam is divided into N elements of the same length $l = L/N$. In the figure, frame (XOY) is the inertia frame, frames $(x_i o_i y_i)$, $i = 1, 2, \ldots, N$, are the local frames for the N elements. Each of them has the same direction as frame $(x_1 o_1 y_1)$, which rotates with the hub and has its origin o_1 at O. Other notations in the figure are defined as:

L: the length of the flexible beam;

EI: the uniform flexural rigidity of the beam;

ρ: the uniform mass per unit length of the beam;

m: the concentrated mass tip payload;

I_h: the hub inertia;

$\tau(t)$: the torque applied by the motor at the base;

$\theta(t)$: the rotation angle of the hub;

$\vec{r}_i(x_i, t)$: the position vector of a point on the ith element of the beam within frame (XOY);

$\vec{o}_i$: the vector from the origin of frame (XOY) to the origin of frame $(x_i o_i y_i)$, such that $\vec{o}_1 = 0$; and

$y_i(x_i, t)$: the elastic deflection of a point on the ith element measured from the undeformed beam within frame $(x_i o_i y_i)$.

Therefore, for all $i = 1, 2, \ldots, N$, we have the following two equations:

$$\vec{o}_i = \begin{bmatrix} (i-1)l\cos\theta(t) \\ (i-1)l\sin\theta(t) \end{bmatrix} \tag{1}$$

$$\vec{r}_i = \vec{o}_i + T_r \begin{bmatrix} x_i \\ y_i(x_i, t) \end{bmatrix}, 0 \le x_i \le l$$

where T_r is the orthogonal transformation matrix between frames (XOY) and $(x_i o_i y_i)$ given by

$$T_r = \begin{bmatrix} \cos\theta(t) & -\sin\theta(t) \\ \sin\theta(t) & \cos\theta(t) \end{bmatrix} \tag{3}$$

In this article, $\vec{r}_i(x_i, t)$ is used to represent the position of a point on the beam, and a nonlinear dynamic model is obtained. It should be pointed out that if the length of the arc is used to approximate the position of a point on the beam, a linear dynamic model can be obtained because of the linearization process introduced by the arc approximation.[7,19]

From equations (1), (2), and (3), we obtain

$$\begin{aligned} \dot{\vec{r}}_i &= \dot{\vec{o}}_i + \dot{T}_r \begin{bmatrix} x_i \\ y_i(x_i, t) \end{bmatrix} + T_r \begin{bmatrix} \dot{x} \\ \dot{y}_i(x_i, t) \end{bmatrix} \\ &= T_r \begin{bmatrix} 0 \\ (i-1)l\dot{\theta} \end{bmatrix} + T_r \begin{bmatrix} -y_i\dot{\theta} \\ x_i\dot{\theta} + \dot{y}_i \end{bmatrix} \\ &= T_r \begin{bmatrix} -y_i\dot{\theta} \\ [(i-1)l + x_i]\dot{\theta} + \dot{y}_i \end{bmatrix} \end{aligned} \tag{4}$$

Consider the ith element shown in Figure 2. As for the nodes through which we divide the beam into elements, each of them undergoes both translational and rotational displacements at the same time when the beam is rotating. The displacements of two nodes

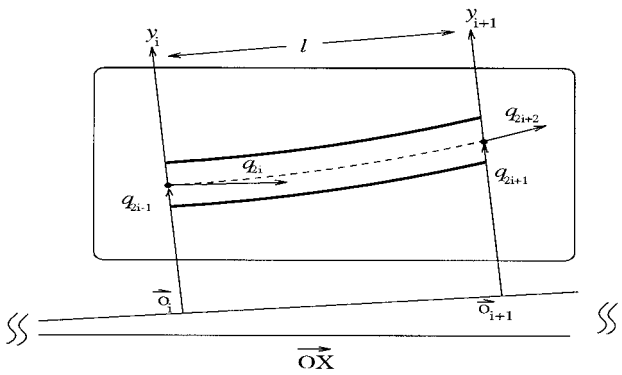

Figure 2. The *i*th element.

of the *i*th element are denoted by q_{2i-1} and q_{2i+1}, and the rotations of the nodes by q_{2i}, q_{2i+2}.

Because there are N elements in total, the number of q_i's is $2N + 2$, i.e., $q_1, q_2, \ldots, q_{2N+2}$. The elastic deflection $y_i(x_i, t)$ for element i can be described by

$$y_i(x_i, t) = \sum_{j=1}^{4} \psi_j(x_i) q_{2(i-1)+j}(t)$$
$$(i = 1, 2, \ldots, N \quad \text{and} \quad 0 < x_i < l) \tag{5}$$

where $\psi_j(x_i)$ are the admissible functions and q_i are generalized coordinates of the system. The boundary conditions at the two nodes of the *i*th element are :[24]

$$\begin{cases} y_i(0, t) = q_{2i-1}(t) \\ \dfrac{\partial y_i(x_i, t)}{\partial x_i}\Big|_{x_i=0} = q_{2i}(t) \\ y_i(l, t) = q_{2i+1}(t) \\ \dfrac{\partial y_i(x_i, t)}{\partial x_i}\Big|_{x_i=l} = q_{2i+2}(t) \end{cases} \tag{6}$$

Assume that the admissible functions ψ_j (j = 1, 2, 3, 4) are the solutions of the differential equation that governs the static bending of the considered beam subject to boundary conditions in (6). Letting $\psi(x)$ be the static elastic deflection, the differential equation of the static bending of the beam is given by[24]

$$\psi''''(x) = 0, \qquad (0 < x < l)$$

The solution of this differential equation has the general form

$$\psi(x) = c_1 x^3 + c_2 x^2 + c_3 x + c_4$$

Recalling (5) and using the boundary conditions in (6), we obtain the four admissible functions[24]

$$\begin{cases} \psi_1(x) = 1 - 3x^2/l^2 + 2x^3/l^3 \\ \psi_2(x) = x - 2x^2/l + x^3/l^2 \\ \psi_3(x) = 3x^2/l^2 - 2x^3/l^3 \\ \psi_4(x) = -x^2/l + x^3/l^2 \end{cases} \tag{7}$$

Let E_{ki} and E_{pi} be the kinetic energy and the potential energy of the *i*th element, and E_{kp} and E_{km} be the kinetic energy of the point mass tip payload and the kinetic energy of the motor. Further, let the generalized coordinate vector of the *i*th element be $Q_i = [\theta\ q_{2i-1}\ q_{2i}\ q_{2i+1}\ q_{2i+2}]^T$, we have

$$E_{ki} = \frac{1}{2}\rho \int_0^l \{\dot{\bar{r}}_i\}^T \{\dot{\bar{r}}_i\}\, dx_i = \frac{1}{2}\dot{Q}_i^T M_i \dot{Q}_i$$

$$E_{pi} = \frac{1}{2} EI \int_0^l \left[\frac{\partial^2 y_i}{\partial x_i^2}\right]^T \left[\frac{\partial^2 y_i}{\partial x_i^2}\right] dx_i = \frac{1}{2} Q_i^T K_i Q_i$$

$$E_{kp} = \frac{1}{2} m \{\dot{\bar{r}}_i|_{i=N, x_i=1}\}^T \{\dot{\bar{r}}_i|_{i=N, x_i=1}\} = \frac{1}{2}\dot{Q}_N^T M_p \dot{Q}_N$$

$$E_{km} = \frac{1}{2} I_h \dot{\theta}^2$$

where M_i is the symmetric and positive definite inertia matrix corresponding to the *i*th element, K_i is the symmetric stiffness matrix of the *i*th element, and M_p is the inertia matrix corresponding to the payload and given by

$$M_p = \begin{bmatrix} d_p & 0 & 0 & Lm & 0 \\ 0 & 0 & 0 & 0 & 0 \\ 0 & 0 & 0 & 0 & 0 \\ Lm & 0 & 0 & m & 0 \\ 0 & 0 & 0 & 0 & 0 \end{bmatrix} \tag{8}$$

where

$$d_p = mL^2 + mq_{2N+1}^2 = mL^2 + my_{tip}^2 \tag{9}$$

Indeed, the first column and the first row of K_i contain only zeros because the potential energy, E_{pi}, is independent of θ. The detailed process of calculating M_i and K_i can be found in refs. 6 and 24. Since the beam is clamped on the rotor of the motor, we have q_1 and

$q_2 \equiv 0$ and subsequently $\dot{q}_1 = \dot{q}_2 \equiv 0$. Thus they can be removed from the above energies. After some algebraic manipulations, the total kinetic energy and the total potential energy of the system can be written into the form

$$E_k = \sum_{i=1}^{N} E_{ki} + E_{kp} + E_{km} = \frac{1}{2}\dot{q}^T M(q)\dot{q} \tag{10}$$

$$E_p = \sum_{i=1}^{N} E_{pi} = \frac{1}{2} q^T K q \tag{11}$$

where $q = [\theta\ q_3 \cdot \cdot \cdot q_{2N+2}]^T \in R^{2N+1}$ is the complete generalized coordinate vector, $M(q)$ is the inertia matrix of the system, which is symmetric and positive definite, and K is the constant symmetric stiffness matrix. In the derivation of $M(q)$ and K in equations (10) and (11), we need to expand M_i, M_p and K_i into square matrices of dimension $2N + 1$. The detailed process has been given in ref. 24. Using the well known *Lagrange-Euler Equation*

$$\frac{d}{dt}\left(\frac{\partial \mathcal{L}}{\partial \dot{q}}\right) - \frac{\partial \mathcal{L}}{\partial q} = T \tag{12}$$

where T is the generalized force vector and $\mathcal{L} = E_k - E_p$ is the *Lagrangian*, we have the following dynamic equation

$$M(q)\ddot{q} + C(q, \dot{q})\dot{q} + Kq = b\tau \tag{13}$$

where $\tau \in R$, $b = [1\ 0 \cdot \cdot \cdot 0]^T \in R^{2N+1}$ and the jkth element, c_{jk}, of matrix $C(q, \dot{q})$ is given by

$$c_{jk} = \sum_{i=1}^{2N+1} \frac{1}{2}\left(\frac{\partial m_{kj}}{\partial u_i} + \frac{\partial m_{ki}}{\partial u_j} - \frac{\partial m_{ij}}{\partial u_k}\right)\dot{u}_i \tag{14}$$

with m_{ij} denotes the ijth element of $M(q)$, and $u_1 = \theta$, $u_2 = q_3, \ldots, u_{2N+1} = q_{2N+2}$. It is easy to check that such a $C(q, \dot{q})$ implies that $\dot{M}(q) - 2C(q, \dot{q})$ is skew-symmetric. By letting

$$X = [q^T\ \dot{q}^T]^T = [\theta\, q_3 \cdot \cdot \cdot q_{2N+2}\ \dot{\theta}\ \dot{q}_3 \cdot \cdot \cdot \dot{q}_{2N+2}]^T \in R^{4N+2}$$

the system can be expressed in state-space form as

$$\dot{X} = AX + B\tau \tag{15}$$

where

$$A = \begin{bmatrix} 0 & I \\ -M^{-1}K & -M^{-1}C \end{bmatrix}, B = \begin{bmatrix} 0 \\ M^{-1}b \end{bmatrix} \tag{16}$$

It should be noted that all the elements except the first one, m_{11}, of $M(q)$ are constants. The m_{11} consists of a constant part and a variable part. Let $Q_i = [q_{2i-1}\ q_{2i}\ q_{2i+1}\ q_{2i+2}]^T$, then m_{11} is given by

$$m_{11} = I_h + d_p + d_q(\bar{Q}_i) \tag{17}$$

in which d_p, given by (9), is the part contributed by the tip payload, and d_q, contributed by the N elements, is a positive scalar function of Q_i in the following quadratic form

$$d_q(\bar{Q}_i) = \sum_{i=1}^{n} \bar{Q}_i^T \begin{bmatrix} \sigma_i^1 & m_i^{12} & m_i^{13} & m_i^{14} \\ m_i^{12} & \sigma_i^2 & m_i^{23} & m_i^{24} \\ m_i^{13} & m_i^{23} & \sigma_i^3 & m_i^{34} \\ m_i^{14} & m_i^{24} & m_i^{34} & \sigma_i^4 \end{bmatrix} \bar{Q}_i \tag{18}$$

where, as stated above, $q_1 = q_2 = 0$, and m_i^{jk} and σ_i^j are given by

$$m_i^{jk} = \rho \int_0^l \psi_j(x_i)\, \psi_k(x_i)\, dx_i$$

$$\sigma_i^j = \rho \int_0^i \psi_j^2(x_i)\, dx_i$$

$$i = 1, 2, \cdot \cdot \cdot, N$$

$$j, k = 1, 2, 3, 4 \text{ and } j < k$$

Such a structure of $M(q)$ is very attractive in helping us to achieve on-line computation of M^{-1}, as will be shown in Appendix A. Subsequently, $C(q, \dot{q})$ has nonzero elements only in its first row and its first column.

3. CONTROLLER DESIGN

In the nonlinear dynamic model obtained above, all elements of the state vector have physical meanings (hub rotation angle and its velocity, displacements and rotations of nodes and their velocities), and can thus be measured or estimated. For example, some LEDs can be mounted at the nodes of the beam, and the vision positioning system introduced in ref. 26, constructed by using a CCD camera overseeing the whole working-space, can be utilized to detect the

position of the nodes. Then, the rotations of the nodes can be approximated from the displacements feedback, and the velocity signals can be estimated from position signals by the backward-difference operator. Obviously, the accuracy of the estimation of nodes' rotations can be improved when the beam is divided into more elements. The system parameters can be measured or calculated. Therefore, in the article, we make the following assumptions:

- **A1:** All the states are obtainable for feedback control either by direct measurement or by estimation.
- **A2:** All the system parameters, such as I_h, L, EI, ρ, and payload, etc., are given for controller design.

From assumptions **A1** and **A2**, we know that $M(q)$, $C(q, \dot{q})$, and K in (13), subsequently A and B in (15), are known. Let us decompose M into $M = M_0 + \Delta M$, where M_0 is the constant part (when the beam is at the equilibrium position) of M under nominal payload condition, and ΔM is the difference between M and M_0, and is of the form

$$\Delta M = \begin{bmatrix} \delta d_p + d_q & 0 & \cdots & 0 & L \cdot \delta m & 0 \\ 0 & 0 & \cdots & 0 & 0 & 0 \\ \vdots & \vdots & & \vdots & \vdots & \vdots \\ L \cdot \delta m & 0 & \cdots & 0 & \delta m & 0 \\ 0 & 0 & \cdots & 0 & 0 & 0 \end{bmatrix} \quad (19)$$

where $\delta m = m - m_0$, m is the actual tip payload and m_0 is its nominal value, $\delta d_p = \delta m \cdot L^2 + \delta m \cdot y_{tip}^2$ with $y_{tip} = q_{2N+1}$ and $d_q \geq 0$ given in (18). Because M is always symmetric and positive definite, M_0 is of course symmetric and positive definite. Then, M^{-1} can be written as $M^{-1} = M_0^{-1} + M_\Delta^{-1}$ (note: M_Δ^{-1} is the difference between M^{-1} and M_0^{-1} but not the inverse of ΔM). Accordingly, A and B can be divided into the nominal static parts A_0, B_0, and the changing parts ΔA and ΔB as follows

$$A = A_0 + \Delta A$$
$$B = B_0 + \Delta B$$

where

$$A_0 = \begin{bmatrix} 0 & I \\ -M_0^{-1}K & 0 \end{bmatrix}, \quad B_0 = \begin{bmatrix} 0 \\ M_0^{-1}b \end{bmatrix}$$

$$\Delta A = \begin{bmatrix} 0 & 0 \\ -M_\Delta^{-1}K & -M^{-1}C \end{bmatrix}, \quad \Delta B = \begin{bmatrix} 0 \\ M_\Delta^{-1}b \end{bmatrix}$$

The system can then be described as

$$\dot{X}(t) = [A_0 + \Delta A]X(t) + [B_0 + \Delta B]\tau \quad (20)$$

where (A_0, B_0) is controllable. When the beam is at the equilibrium position and under nominal payload, ΔA and ΔB are all null matrices. The system has been transformed into a combination of linear and nonlinear parts. This is a common practice in controller design for nonlinear systems. A similar partition of M is used in Appendix A for efficient computation of M^{-1}, in which $M = M_0 + \Delta M$ with $\Delta M = \Delta M\,|_{\delta m = m}$, i.e., the M_0 corresponds to the beam at the equilibrium position and with 0 payload. From assumptions **A1** and **A2**, A_0 and B_0, ΔA, and ΔB are known as well.

Motivated by the controller design for mismatched systems given in ref. 25, a robust nonlinear states feedback controller achieving tip position control is constructed here for system (20). Firstly, let us briefly discuss the robust controller given in ref. 25. Consider the uncertain dynamic system described by

$$\dot{X}(t) = [A_0 + \Delta A]X(t) + [B_0 + \Delta B]u$$

where A_0 and B_0 are the nominal parts of the system, and ΔA and ΔB are unknown uncertainties of the system but with known upper bounds, and can be decomposed into matched parts and mismatched parts. The control law given in ref. 25 is

$$u = FX + p_\varepsilon(X) \quad (21)$$

where F is designed such that $\bar{A} = A_0 + B_0F$ is asymptotically stable, and $p_\varepsilon(X)$ is a nonlinear function of the bounds of the matched uncertainties, which, in practice, are usually hard to know exactly. For a given symmetric and positive definite matrix Q, solve for P from the Lyapunov Equation

$$P\bar{A} + \bar{A}^TP = -Q \quad (22)$$

It has been proven[25] that the system's mismatched uncertainties must be covered by the following *mismatched threshold*

$$M^* = \frac{\lambda_{\min}(Q)}{2\lambda_{\max}(P)} \quad (23)$$

to assure the *Practical Stability*[25] of the system. When F is independent of P, M^* has its maximum when $Q = I$.

Under assumptions **A1** and **A2**, A and B, ΔA, and ΔB are all known. A nonlinear feedback controller can then be constructed using ΔA and ΔB themselves, instead of the hard-to-know upper bounds of the matched uncertainties. Suppose the control torque signal has the same form as (21), i.e.,

$$\tau(X, t) = FX + \rho_\varepsilon(X) \tag{24}$$

where F is selected as stated above, i.e., to ensure that $A = A_0 + B_0F$ is asymptotically stable around the equilibrium position, and $p_\varepsilon(X)$ is a nonlinear states feedback expressed in terms of ΔA and ΔB explicitly, as will be shown later.

Substituting (24) into system (20), we have the closed-loop dynamic equation as

$$\dot{X} = \bar{A}X + (\Delta A + \Delta BF)X + Bp_\varepsilon(X) \tag{25}$$

The closed-loop stability of the system is stated in the theorem below.

Theorem: *The closed-loop system* (25) *is asymptotically stable if, for* $\varepsilon > 0$, $p_\varepsilon(X)$ *is designed as*

$$p_\varepsilon(X) = \begin{cases} -\dfrac{B^TPX}{\|B^TPX\|^2} X^T P(\Delta A + \Delta BF)X & \text{when } \|B^T PX\|^2 \geq \varepsilon \\ -\dfrac{B^TPX}{\varepsilon} X^T P(\Delta A + \Delta BF)X & \text{when } \|B^T PX\|^2 < \varepsilon \end{cases} \tag{26}$$

and when $\|B^TPX\|^2 < \varepsilon$, *the changing parts of the system,* ΔA *and* ΔB, *satisfy the following inequality*

$$\|\Delta A + \Delta BF\| < \frac{\lambda_{\min}(Q)}{2\lambda_{\max}(P)} = M^* \tag{27}$$

where $P^T = P > 0$ *is the solution of the Lyapunov Equation* (22).

Proof: Select the Lyapunov Candidate as

$$V(X) = X^T PX \tag{28}$$

The derivative of $V(X)$ along the closed-loop dynamic equation (25) is given by

$$\begin{aligned} \dot{V}(X) &= 2X^TP[(\bar{A}X + (\Delta A + \Delta BF)X + Bp_\varepsilon(X)] \\ &= -X^TQX + 2X^T P[(\Delta A + \Delta BF)X + Bp_\varepsilon(X)] \end{aligned} \tag{29}$$

When $\|B^T PX\|^2 \geq \varepsilon$, we have

$$\dot{V}(X) = -X^TQX \tag{30}$$

which is negative definite, and when $\|B_TPX\|^2 < \varepsilon$, we have

$$\begin{aligned} \dot{V}(X) &= -X^TQX + 2X^T P(\Delta A + \Delta BF)X - 2\frac{\|B^T PX\|^2}{\varepsilon} \\ &\quad X^T P(\Delta A + \Delta BF)X \\ &= -X^T QX + 2\left(1 - \frac{\|B^T PX\|^2}{\varepsilon}\right) X^T P(\Delta A + \Delta BF)X \\ &\leq -\lambda_{\min}(Q))\|X\|^2 + 2\lambda_{\max}(P)\|X\|^2\|\Delta A + \Delta BF\| \end{aligned}$$

From (27), i.e., $2\lambda_{\max}(P)\|\Delta A + \Delta BF\| < \lambda_{\min}(Q)$, we have $\dot{V}(X) < 0$. Thus, with $p_\varepsilon(X)$ given in (26) and under the inequality (27), the closed-loop system is asymptotically stable. ■

Obviously, it is desirable to maximize the *mismatched threshold*, M^* in (27) for a robust controller. In ref. 25, it was mentioned that M^* has its maximum when $Q = I$. Actually, it is easy to show that $Q = aI$ ($a > 0$) will give the same maximum value of M^*. However, it should be pointed out that this is valid only when F is independent of P. If F is selected to be a function of P, such as $F = -\frac{1}{2}R^{-1}B_0^TP$ as suggested in ref. 25, then the Lyapunov Equation (22) becomes the following Riccati Equation

$$A_0^TP + P A_0 - PB_0R^{-1}B_0^TP + Q = 0 \tag{31}$$

Using the example in ref. 25, in which the nominal parts of the system were chosen as

$$(A_0, B_0) = \left(\begin{bmatrix} 0 & 1 \\ 1 & 0 \end{bmatrix} \begin{bmatrix} 0 \\ 3 \end{bmatrix}\right) \tag{32}$$

and $R = 2$, solving (31) with $Q = aI(a > 0)$, we found

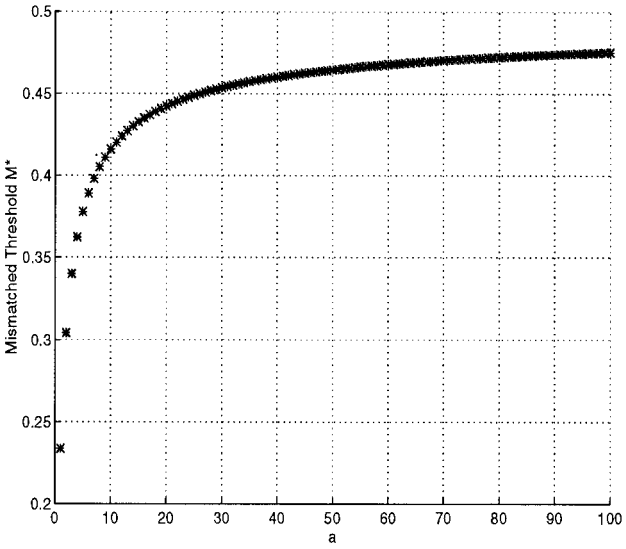

Figure 3. Mismatched threshold M^* with $Q = aI$.

that M^* increases with a as shown in Figure 3. Therefore, when F is dependent on P, to obtain a proper M^*, one should not only consider the bounds of the system uncertainties, but also the acceptability of Q, since it affects the choice of P and subsequently the final controller.

As shown above, by using the FEM model, the robust controller in ref. 25 has been changed into a nonlinear states feedback controller (24), with $p_\varepsilon(X)$ given in (26). For the robust controller in ref. 25, the use of bounds of system's uncertainties (which are usually difficult to know) may cause the control signal to be unnecessarily large, while, for our nonlinear feedback controller, the direct use of system matrices can be expected to generate a smoother control torque. To implement the nonlinear feedback controller, we need to find an efficient way to calculate ΔA, ΔB, and B on-line. By checking (16), one can find that most of the computation is for obtaining the inverse of the system inertia matrix M. For this, an efficient algorithm is developed in Appendix A to achieve on-line computation of M^{-1}.

4. NUMERICAL SIMULATIONS

Numerical simulations have been carried out to verify the effectiveness of the nonlinear feedback controller. To obtain more persuasive results, the plant is obtained with six elements, i.e., $N = 6$, and the controller is designed based on a two-element model. This implies that a controller based on a comparatively rough model is used to control a more accurate model. The system parameters are given such values as: $L = 1.0$ m, $Ih = 0.05$ Kg^2, $EI = 2.0$ Nm^2, and $\rho = 0.1$ kg/m. The tip position is defined as $L\theta + y_{tip}$. The terminal joint position is set to be $\theta = \pi/2$ rad. The small positive scalar ε is selected to be 0.01. The linear states feedback matrix F is calculated by $F = -\frac{1}{2}R^{-1}B_0^T P$ as in ref. 25 with $R = 1$, $Q = I$, and P is the solution of (31). From the numerical analysis in section 3, we know what if F is dependent on P, the selection of $Q = I$ may not ensure the *mismatched threshold* M^* to be maximized. The simulations are presented here only for illustration purpose.

First, the mass of the tip payload is assumed to be exactly known. The simulation results for $m = m_0 = 0.1$ kg and 0.5 kg are shown in Figure 4 and Figure 5, respectively. It can be seen that when the mass of the payload is five times as heavy as the beam, the controller still can assure rather fast convergence speed.

Then, unknown payload is considered to test the robustness of the controller in handing payload variations. Indeed, the payload of a robot in practice is often unknown or undergoes unknown changes. In this case, the system matrices for controller design are obtained by just using the nominal payload. The controller showed perfect robustness in handling the changes in payload in the following simulations. The nominal payload m_0 was chosen to be 0.1 kg, and the actual payload m was first selected to be 0.2 kg, i.e., double the nominal value, and then a heavier one $m = 0.5$ kg. Figure 6 and Figure 7 show the comparison of tip deflections and tip positions between the known payload case and the unknown payload case. One can see that the results when m is known and when it is unknown are very close. Furthermore, to show the comparison results clearly, the errors of tip deflections and of tip positions are given in Figure 8 and Figure 9. It can be seen that the proposed nonlinear feedback controller is very robust to payload variations, and the controller obtained from the nominal payload is able to handle the payload changes in a rather large range.

5. CONCLUSION

In this article, we discussed the modeling of a one-link flexible manipulator using the finite element method (FEM), and a nonlinear dynamic model was obtained. The nonlinearity is introduced by the fact that the inertial matrix M has its first element

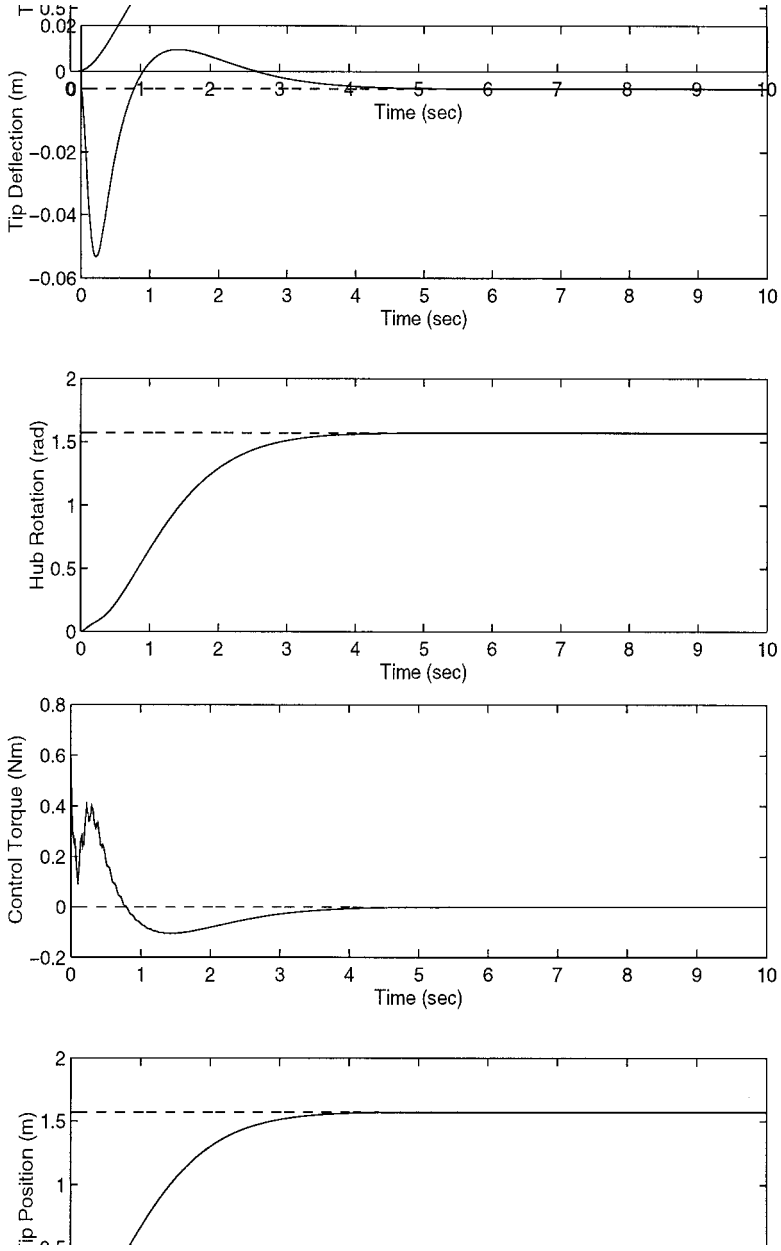

Figure 4. Control performance when $m = m_0 = 0.1$ kg (the weight of beam).

m_{11} as a function of the generalized coordinates of the system. The controller presented in ref. 25 was also briefly discussed, and problems existing in maximizing the *mismatched threshold* M^* was analyzed numerically as well. Motivated by the work presented in ref. 25, an effective nonlinear states feedback controller was constructed for the flexible robot system. To realize the controller, an efficient algorithm was developed to achieve on-line computation of M^{-1}. Intensive numerical simulation results were given to show that the controller works well and is very robust to payload variations.

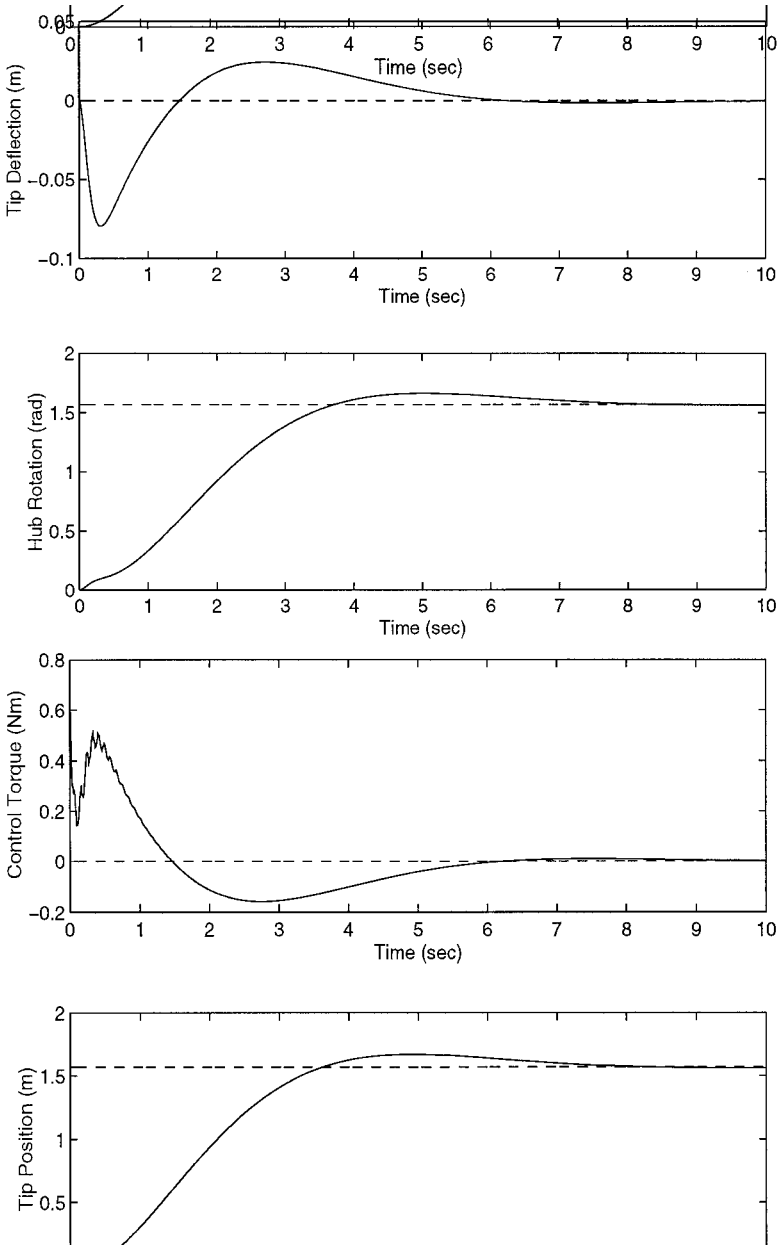

Figure 5. Control performance when $m = m_0 = 0.5$ kg (5 times the weight of beam).

APPENDIX A: ON-LINE COMPUTATION OF M^{-1}

The main difficulty in realizing the controller introduced in section 3 is that we must be able to obtain system matrices ΔA, ΔB, and B on-line to implement τ. Most of the computation is for obtaining the inverse of the system inertia matrix M^{-1}. In general, computation of the inverse of a matrix is very time-consuming, especially when the size of the matrix is large. A fast computation method to compute M^{-1} is given below by using the following Matrix Inverse Lemma.

Matrix Inverse Lemma: *Let A, C, and $C^{-1} + DA^{-1}B$ be nonsingular square matrices, then*

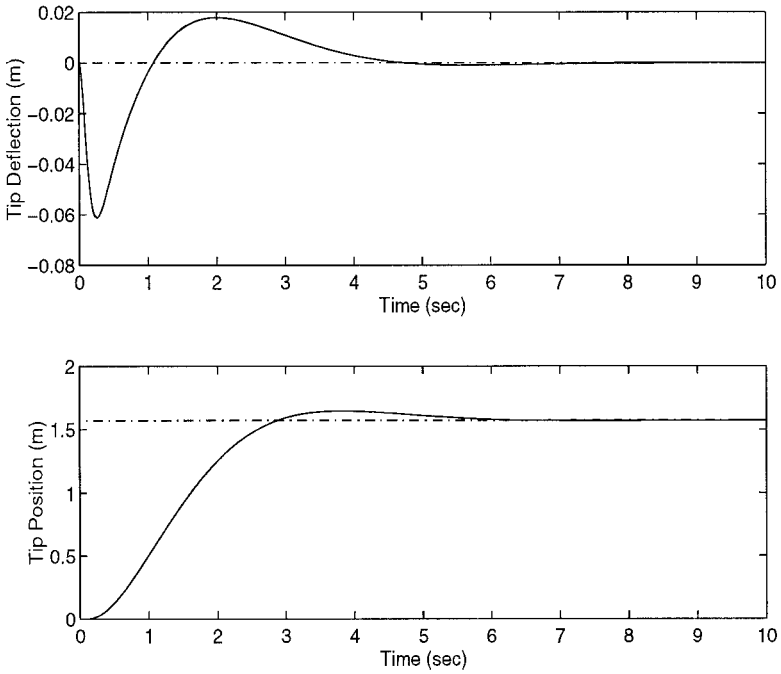

Figure 6. Control performance when $m = 2m_0 = 0.2$ kg (twice the weight of beam).

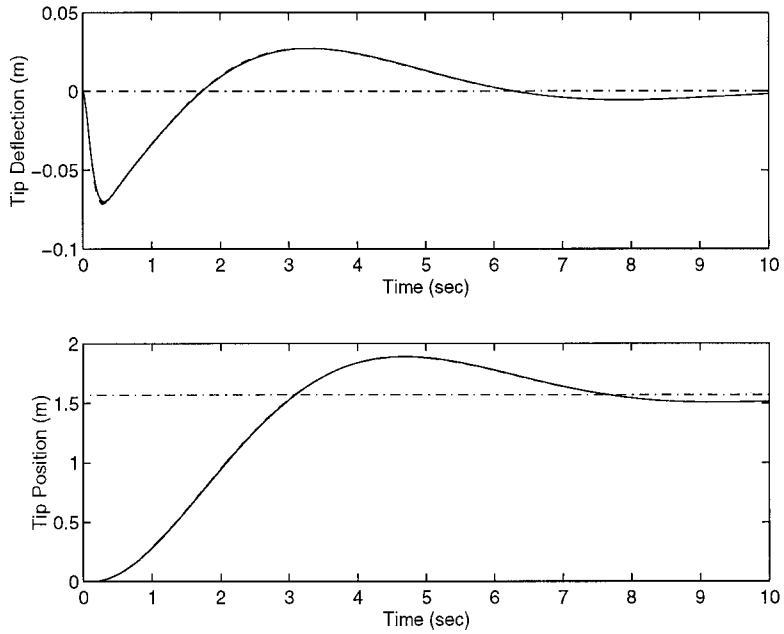

Figure 7. Control performance when $m = 5m_0 = 0.5$ kg (5 times the weight of beam).

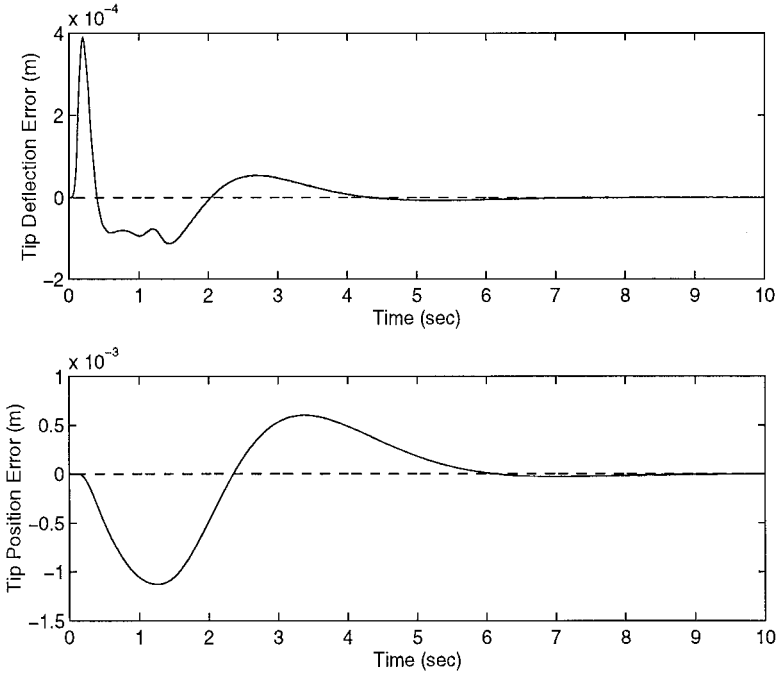

Figure 8. Error between known and unknown payload cases when $m = 2m_0 = 0.2$ kg.

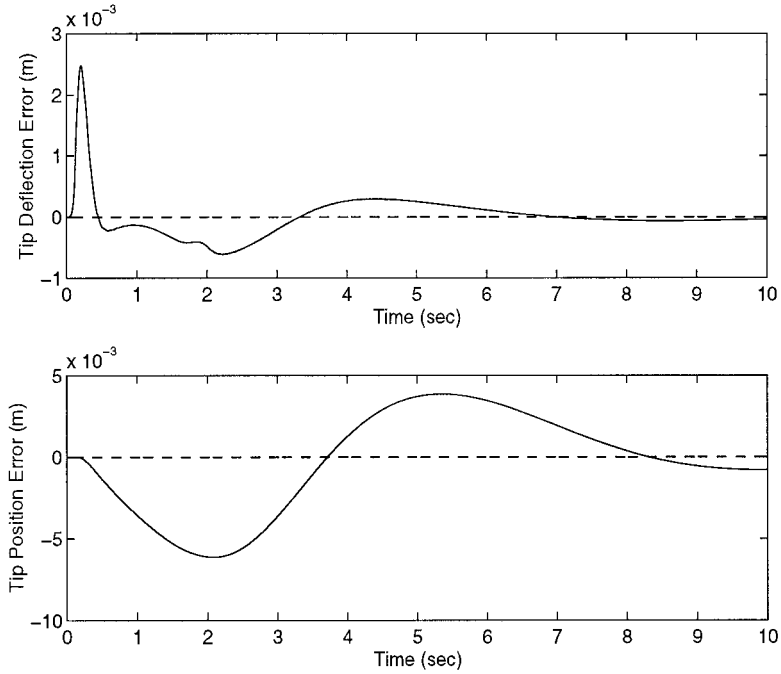

Figure 9. Error between known and unknown payload cases when $m = 5m_0 = 0.5$ kg.

$$(A + BCD)^{-1} = A^{-1} - A^{-1}B(C^{-1} + DA^{-1}B)^{-1}DA^{-1} \tag{33}$$

Proof: Multiplying both sides by $A + BCD$, the identity can be verified.

To use the above lemma in our computation, we first decompose M as

$$M = \bar{M}_0 + \Delta\bar{M} \tag{34}$$

where $\bar{M}_0$ is the constant part corresponding to the beam at the equilibrium position and with *zero* payload, and ΔM is the difference between M and $\bar{M}_0$. Thus, $\bar{M}_0$ is symmetric and positive definite, and ΔM can be written as

$$\Delta\bar{M} = \begin{bmatrix} d_p + d_q & 0 & \cdots & 0 & L \cdot m & 0 \\ 0 & 0 & \cdots & 0 & 0 & 0 \\ \vdots & \vdots & \vdots & & \vdots & \vdots \\ L \cdot m & 0 & \cdots & 0 & m & 0 \\ 0 & 0 & \cdots & 0 & 0 & 0 \end{bmatrix} \tag{35}$$

where m is the actual tip payload, and d_p and d_q are given by (9) and (18), respectively. Note that $\bar{M}_0 \neq M_0$ and $\Delta\bar{M} \neq \Delta M$. $\bar{M}_0$ and $\Delta\bar{M}$ are used for controller design, while M_0 and ΔM are introduced to solve the problem of fast computation of M^{-1}.

Introducing $d_1 = [\sqrt{d_q + m \cdot y_{tip}^2}\ 0 \cdots 0]^T \in R^{2N+1}$ and $d_2 = [L\ 0 \cdots 0\ 1\ 0]^T \in R^{2N+1}$, we have

$$\Delta\bar{M} = d_1 \cdot d_1^T + d_2 \cdot m \cdot d_2^T$$

and subsequently M can be written as

$$M = \bar{M}_0 + d_1 \cdot d_1^T + d_2 \cdot m \cdot d_2^T$$

Because the tip payload $m \geq 0$, the term $\sqrt{d_q + m \cdot y_{tip}^2}$ in d_1 is always well-defined. If the partition $M = \bar{M}_0 + \Delta M$, instead of (34) is used, then the corresponding term in d_1 becomes $\sqrt{d_q + \delta m \cdot y_{tip}^2}$, which may not be well-defined in the case when $\delta m < 0$ (i.e., when the actual payload is lighter than the nominal payload). $\bar{M}_0$ is symmetric and positive definite, so is $\bar{M}_0^{-1}$. Therefore $1 + d_1^T \bar{M}_0^{-1} d_1 > 0$. From the Matrix Inverse Lemma, we have

$$\begin{aligned} \Gamma(q, m) &:= (\bar{M}_0 + d_1 \cdot d_1^T)^{-1} \\ &= \bar{M}_0^{-1} - \bar{M}_0^{-1} d_1 (1 + d_1^T \bar{M}_0^{-1} d_1)^{-1} d_1^T \bar{M}_0^{-1} \end{aligned}$$

Obviously $\Gamma(q, m)$ is symmetric and positive definite as well. When $m = 0$, i.e., the no payload case, we have $M^{-1} = \Gamma(q, 0)$. Simarly, taking $\bar{M}_0 + d_1 \cdot d_1^T$ as the matrix A in the lemma, we have

$$\begin{aligned} M^{-1} &= [(\bar{M}_0 + d_1 \cdot d_1^T) + d_2 \cdot m \cdot d_2^T]^{-1} \\ &= \Gamma - \Gamma d_2 \left(\frac{1}{m} + d_2^T \Gamma d_2 \right)^{-1} d_2^T \Gamma \end{aligned} \tag{36}$$

Noting that $1/m + d_2^T \Gamma d_2$ is actually a scalar, M^{-1} can be further written into the following form

$$M^{-1} = \Gamma(q, m) - \frac{m}{1 + m d_2^T \Gamma(q, m) d_2} \Gamma(q, m) d_2 d_2^T \Gamma(q, m) \tag{37}$$

which is well-defined for any generalized coordinate vector q and payload m. Because $\bar{M}_0$ is the constant part of M, $\bar{M}_0^{-1}$ can be calculated off-line, and from (37), one can see that no matrix inverse is needed in on-line computation, thus the amount of computation is greatly reduced.

REFERENCES

1. V. V. Korolov and Y. H. Chen, ''Robust control of a flexible manipulator arm,'' *Proc. IEEE Int. Conf. Rob. Autom.*, Philadelphia, 1988, Vol. 1, pp. 159–164.
2. Y. Sakawa, F. Matsuno, and S. Fukushima, ''Modeling and feedback control of a flexible arm,'' *J. Rob. Syst.*, **2**(4), 453–472, 1985.
3. H. Krishnan, ''Bounded input discrete-time control of a single-link flexible beam,'' Master's dissertation, University of Waterloo, Ontario, 1988.
4. D. Wang and M. Vidyasagar, ''Transfer functions for a single flexible link,'' *Proc. IEEE Int. Conf. Rob. Autom.*, Scottsdale, AZ, 1989, pp.l 1042–1047.
5. E. Bayo, ''A finite element approach to control the end-point motion of a single-link flexible robot,'' *J. Rob. Syst.*, **4**(1), 63–75, 1987.
6. P. B. Usoro, R. Nadira, and S. S. Mahil, ''A finite element/lagrange approach to modeling lightweight flexible manipulators,'' *J. Dyn. Syst. Meas. Control Trans. ASME*, **108**(3), 198–205, 1986.
7. S. S. Ge, T. H. Lee, and G. Zhu, ''Comparison studies between assumed modes method and finite element method in modeling a single-link flexible manipulator,'' *Proc. IEEE Int. Conf. Intell. Control Instrum.*, Singapore, 1995, pp. 376–381.
8. K. Zuo and D. Wang, ''Closed loop shaped-input control of a class of manipulators with a single flexible link,'' *Proc. IEEE Int. Conf. Rob. Autom.*, Nice, France, 1992, pp. 782–787.
9. A. Tzes and S. Yurkovich, ''An adaptive input shaping control scheme for vibration suppression in slewing

flexible structures,'' *IEEE Trans. Control Syst. Technol.,* **1,** 114–121, 1993.
10. E. Bayo and H. Moulin, ''An efficient computation of the inverse dynamics of flexible manipulators in time domain,'' *Proc. IEEE Int. Conf. Rob. Autom.,* Scottsdale, AZ, 1989, Vol. 2, pp. 710–715.
11. K. S. Rattan and V. Feliu, ''Feedforward control of flexible manipulators,'' *Proc. IEEE Int. Conf. Rob. Autom.,* Nice, France, 1992, pp. 788–793.
12. F. Khorrami and Umit Ozguner, ''Perturbation methods in control of flexible link manipulators,'' *Proc. IEEE Int. Conf. Rob. Autom.,* Philadelphia, 1988, Vol. 1, pp. 310–315.
13. B. Siciliano and W. J. Book, ''A singular perturbation approach to control of lightweight flexible manipulators,'' *Int. J. Rob. Res.,* **7**(4), 79–90, 1988.
14. T. C. Yang, J. C. S. Yang, and P. Kudva, ''Load-adaptive control of a single-link flexible manipulator,'' *IEEE Trans. Syst. Man Cybern.,* **22**(1), 85–91, 1992.
15. D. C. Nemir, A. J. Koivo, and R. L. Kashyap, ''Pseudolinks and the self-tuning control of a nonrigid link mechanism,'' *IEEE Trans. Syst. Man Cybern.,* **18**(1), 40–48, 1988.
16. B. Siciliano, B. S. Yuan, and W. J. Book, ''Model reference adaptive control of a one link flexible arm,'' *Proc. IEEE Int. Conf. Decis. Control,* Athens, Greece, 1986, pp. 91–95.
17. B. S. Yuan, W. J. Book, and B. Siciliano, ''Direct adaptive control of a one-link flexible arm with tracking,'' *J. Rob. Syst.,* **6**(6), 663–680, 1989.
18. V. Feliu, K. S. Rattan, and H. B. Brown, Jr., ''Adaptive control of a single-link flexible manipulator,'' *IEEE Control Syst. Mag.,* **10,** 29–33, 1990.
19. C. H. Menq and J. S. Chen, ''Dynamic modeling and payload-adaptive control of a flexible manipulator,'' *Proc. IEEE Int. Conf. Rob. Autom.,* Philadelphia, 1988, Vol. 1, pp. 488–493.
20. C. Canudas de Wit and E. Van den Bossche, ''Adaptive control of a flexible arm with explicit estimation of the payload mass and friction,'' *IFAC Theory of Robots,* Vienna, Austria, 1986, pp. 277–282.
21. D. M. Rovner and G. F. Franklin, ''Experiments in load-adaptive control of a very flexible one-link manipulator,'' *Automatica,* **24**(4), 541–548, 1988.
22. Y. P. Yang and J. S. Gibson, ''Adaptive control of a manipulator with a flexible link,'' *J. Rob. Syst.,* **6**(3), 217–232, 1989.
23. Y. Aoustin, C. Chevallereau, A. Glumineau, and C. H. Moog, ''Experimental results for the end-effector control of a single flexible robotic arm,'' *IEEE Trans. Control Syst. Technol.,* **2**(4), 371–381, 1994.
24. L. Meirovitch, *Elements of Vibration Analysis,* McGraw-Hill, New York 1975, Ch. 5, 8.
25. Y. H. Chen, ''On the robustness of a mismatched uncertain dynamical system,'' *J. Dyn. Syst. Meas. Control Trans. ASME,* **109,** 29–35, 1987.
26. R. H. Cannon, Jr. and E. Schmitz, ''Initial experiments on the end-point control of a flexible one-link robot,'' *Int. J. Rob. Res.,* **3**(3), 62–75, 1984.